

The Integrated Sachs-Wolfe Effect in Interacting Dark Energy Models

Germán Olivares*,¹ Fernando Atrio-Barandela†,² and Diego Pavón‡¹

¹*Departamento de Física, Universidad Autónoma de Barcelona, Barcelona, Spain*

²*Departamento de Física Fundamental, Universidad de Salamanca, Spain*

Models with dark energy decaying into dark matter have been proposed in Cosmology to solve the coincidence problem. We study the effect of such coupling on the cosmic microwave background temperature anisotropies. The interaction changes the rate of evolution of the metric potentials, the growth rate of matter density perturbations and modifies the Integrated Sachs-Wolfe component of cosmic microwave background temperature anisotropies, enhancing the effect. Cross-correlation of galaxy catalogs with CMB maps provides a model independent test to constrain the interaction. We particularize our analysis for a specific interacting model and show that galaxy catalogs with median redshifts $z_m = 0.1 - 0.9$ can rule out models with an interaction parameter strength of $c^2 \simeq 0.1$ better than 99.95% confidence level. Values of $c^2 \leq 0.01$ are compatible with the data and may account for the possible discrepancy between the fraction of dark energy derived from WMAP 3yr data and the fraction obtained from the ISW effect. Measuring the fraction of dark energy by these two methods could provide evidence of an interaction.

I. INTRODUCTION

Measurements of luminosity distances using supernovae type Ia (SNIa) [1], of the cosmic microwave background (CMB) temperature anisotropies with the WMAP satellite [2], large scale structure [3, 4], the integrated Sachs-Wolfe effect [5, 6], and weak lensing [7], indicate that the Universe has entered a phase of accelerated expansion -see [8] for recent reviews. This acceleration is explained in terms of an unknown and nearly unclustered matter component of negative pressure, dubbed “dark energy” (energy density, ρ_x), that currently contributes with about 75% of the total density. The remaining 25% is shared between cold dark matter ($\rho_c \sim 21\%$), baryons ($\rho_b \sim 4\%$), and negligible amounts of relativistic particles (photons and neutrinos). The pressureless non-relativistic matter component redshifts faster with expansion than the dark energy, giving rise to the so-called ‘coincidence problem’ that seriously affects many models of late acceleration, particularly the Λ CDM model: “Why are matter and dark energy densities of the same order precisely today?” [9]. To address this problem within general relativity one must either accept an evolving dark energy field or adopt an incredibly tiny cosmological constant and admit that the “coincidence” is just that, a coincidence that might be alleviated by turning to anthropic ideas [10]. (It should be mentioned, however, the existence of proposals in which a vacuum energy density of about the right order of magnitude arises from the Casimir effect at cosmic scales -see [11] and references therein).

One way to address the coincidence problem, within general relativity, is to assume an interaction (coupling) between the dark energy component and cold dark matter such that the ratio $r \equiv \rho_c/\rho_x$ evolves from a constant but unstable value at early times (in the radiation and matter dominated epochs) to a lower, constant and stable attractor at late times well in the accelerated expansion era [12, 13]. Before the late accelerated expansion was observed, Wetterich introduced interacting quintessence models to reduce the theoretical high value of the cosmological constant [14]. Later, these kind of models were rediscovered, sometimes (but not always) in connection with the coincidence problem -see, e.g. [15]. Other solutions (known as $f(R)$ models) require the Einstein-Hilbert action to be modified [16].

Interacting quintessence models are testable since they predict differences in the expansion rates of the Universe, the growth of matter density perturbations, the Cosmic Microwave Background (CMB) temperature

* E-mail address: german.olivares@uab.es

† E-mail address: atrio@usal.es

‡ E-mail address: diego.pavon@uab.es

anisotropies and in other observables. In this paper we shall demonstrate that, as the Integrated Sachs-Wolfe effect measures directly the growth rate of matter density perturbations, can be used to detect variations on the evolution of the large scale structure with respect to the prediction of the concordance Λ CDM model. As a toy model, we shall consider a spatially flat Friedmann–Robertson–Walker universe filled with radiation, baryons, dark matter and dark energy such that the last two components interact with each other through a coupling term, $Q = 3\mathcal{H}c^2(\rho_c + \rho_x)$. Thus, the energy balance equations for dark matter and dark energy take the form

$$\dot{\rho}_c + 3\mathcal{H}\rho_c = 3\mathcal{H}c^2(\rho_c + \rho_x), \quad \dot{\rho}_x + 3\mathcal{H}(1 + w_x)\rho_x = -3\mathcal{H}c^2(\rho_c + \rho_x), \quad (1)$$

where $w_x = p_x/\rho_x < -1/3$ is the equation of state parameter of the dark energy component and c^2 is a constant parameter that measures the strength of the interaction (it should not be confused with the speed of light that we set equal to unity). Derivatives are taken with respect to the conformal time, and $\mathcal{H} = \dot{a}/a$, with a the scale factor of the Friedmann–Robertson–Walker metric. To satisfy the severe constraints imposed by local gravity experiments [17, 18], baryons and radiation couple to the other two energy components only through gravity. Our ansatz for Q guarantees that the ratio between energy densities, r , tends to a fixed, attractor, value at late times. It yields a constant but unstable ratio at early times. The details of the calculation can be found in [13, 19, 20, 21]. This result holds irrespective of whether the dark energy is a quintessence (i.e., $-1 < w_x < -1/3$), phantom ($w_x < -1$), k -essence or tachyon scalar field [22]. It is worth to remark that the above ansatz implies an effective power law potential for the quintessence dark energy field at early times and an effective exponential potential at late times [12].

Beyond the physical motivation for the existence of a coupling between dark matter and dark energy, their interaction parameter c^2 needs to be constrained by observations. In [20] we showed that the slope of the matter power spectrum at small scales decreases and the scale of matter radiation equality is shifted to larger scales with the interaction. CMB temperature anisotropies are equally affected if the interaction is present at decoupling. The luminosity distance of SNIa depends on the expansion rate of the Universe and can be used to test the existence of a DM/DE coupling. Comparison of model predictions with data showed that only WMAP 3yr data and the Sloan Digital Sky Survey (SDSS) data provided constraints on the value of c^2 [20, 21]. In particular, the SNIa data proved to be rather insensitive to the coupling. In this paper we show that the Integrated Sachs-Wolfe (ISW) component of the CMB temperature anisotropies is much more sensitive than the SNIa data at redshifts $z \sim 1$. It measures the growth factor of linear matter density perturbations, that is strongly affected by the interaction and can effectively set constraints on Interacting Quintessence Models (IQM). Other experiments that also constrain the growth rate are discussed in [23]. In Section II we briefly summarize the formalism behind the measurements of the ISW effect by cross-correlating CMB data with galaxy catalogs. In Section III we describe the observational prospects and in Section IV we present our conclusions.

II. THE INTEGRATED SACHS-WOLFE EFFECT

When CMB photons in their way to the observer from the surface of last scattering, cross a time-varying potential well, experience the so called late Integrated Sachs-Wolfe effect. Photons are blueshifted (redshifted) when entering (leaving) a high dense region, and similarly for low dense regions. If the gravitational potential ϕ evolves during a photon crossing like in models with a cosmological constant, then both effects will not compensate each other and the final energy of the photon will vary. The net effect will be [24],

$$\frac{\Delta T_{ISW}(\hat{n})}{T_0} = -2 \int_0^{r_{rec}} dr \frac{\partial \phi(r, \hat{n})}{\partial r}. \quad (2)$$

The integral is taken with respect to conformal distance (or look-back time) from the observer at redshift $z = 0$, $r(z) = \int_0^z dz'/H(z')$ where the Hubble factor, H , obeys Friedmann's equation, $3H^2 = 8\pi G(\rho_c + \rho_x)$.

The evolution of the Newtonian potential will be computed numerically, but its qualitative behavior can be understood from the perturbed Einstein's equations. Once the Universe becomes matter dominated, we can

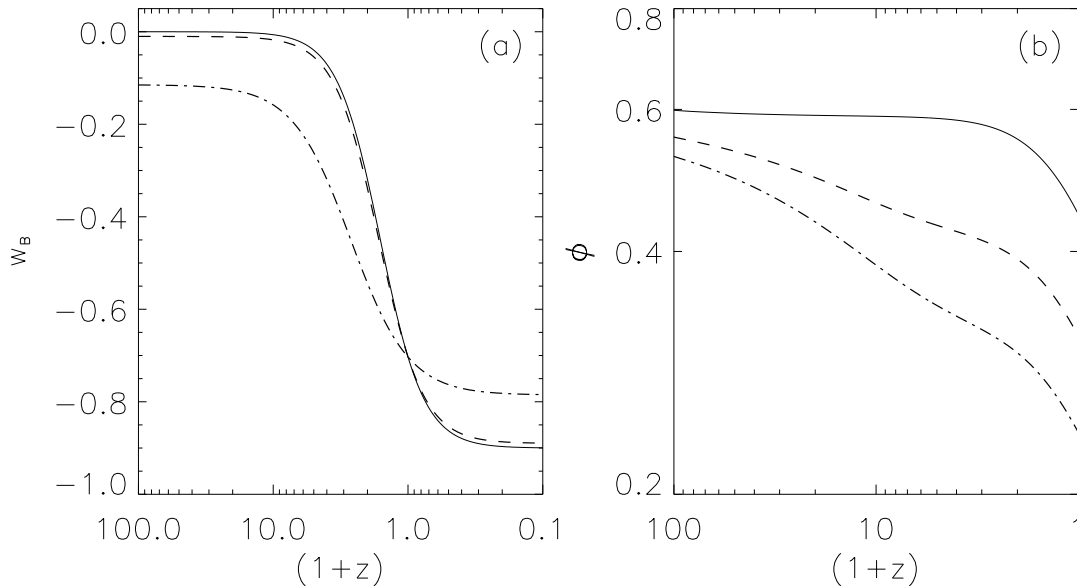


FIG. 1: Panel (a): Evolution of the background equation of state parameter, w_B , as a function of redshift. Panel (b): Evolution of the Newtonian potential ϕ for the wavenumber mode $k = 0.01 h \text{ Mpc}^{-1}$. Solid, dashed and dot-dashed lines correspond to $c^2 = 0, 0.01$, and 0.1 , respectively. In drawing the figures we have set $w_x = -0.9$.

write in the conformal Newtonian gauge [20, 25]:

$$\ddot{\phi} + \mathcal{H}\dot{\phi} - 3w_B\mathcal{H}^2\phi = \frac{3}{2}\mathcal{H}^2 \sum_i \left(\frac{\delta P_i}{\delta \rho_i} \right)^2 \delta_i \Omega_i, \quad (3)$$

where the sum is over all matter fluids and scalar fields, Ω_i , δ_i are the density parameter and the energy density contrast, respectively, of fluid i . Derivatives are also taken with respect to conformal time. In non-interacting models, the gravitational potential changes when (a) the equation of the state of the background varies, and (b) the dark energy is smoothly distributed, i.e., it does not cluster on scales below the “sound horizon”, set by $c_{s,x}^2 = (\delta P_x / \delta \rho_x)$. At that point the potential will decay and generate an ISW effect [26, 27]. During the matter dominated epoch, the matter sound speed is $c_{s,c}^2 = (\delta P_c / \delta \rho_c) = 0$. If $c_{s,x}^2 = 1$, then the dark energy fluid does not cluster on scales below the horizon [28], whereby $\delta_x \sim 0$. In this case, on subhorizon scales the gravitational potential evolves as $\phi = C_1 + C_2 a^{-5/2}$, i.e., it essentially remains constant. However, in models with interaction, the CDM energy density does not scale as a^{-3} because of the coupling. During the matter dominated regime, the background equation of state parameter is $w_B = c^2 w_x / (c^2 + 1) < 0$ and the growing mode in Eq. (3) becomes $\phi = C_1 a^m$ with $m < 3w_B/4 < 0$; that is, there are no growing modes and the potential ϕ decays. In the period of accelerated expansion, in both interacting and non-interacting models, ϕ decays. In Fig. 1a we plot the evolution of w_B as a function of redshift. Solid, dashed and dot-dashed lines correspond to $c^2 = 0, 0.01$, and 0.1 , respectively, and we have set $w_x = -0.9$. Notice that when $c^2 \neq 0$, the matter dominated period has $w_B \neq 0$. In Fig. 1b we depict the time evolution of the Newtonian potential ϕ as a function of redshift for a mode of wavenumber $k = 0.01 h \text{ Mpc}^{-1}$. In the three cases, the amplitude of the potential is normalized to unity at horizon crossing. We solved the system of equations that describes the evolution of all energy components and the Newtonian potentials using a modified version of the CMBFAST code [29]. As the figure shows, when $c^2 = 0$, ϕ remains constant during the matter dominated epoch, and it decays solely during the phase of accelerated expansion. By contrast, in interacting models the potential ϕ decays even during matter domination.

The ISW effect is not the only anisotropy generated by local structures. Secondary anisotropies could be generated due to non-linear evolution of the gravitational potential, usually associated with the gravitational collapse of small scale structures like clusters [30]. But the relevant scales are those of clusters and superclusters, corresponding to angular scales of $5 - 10$ arcmin, much smaller than those associated to the ISW effect.

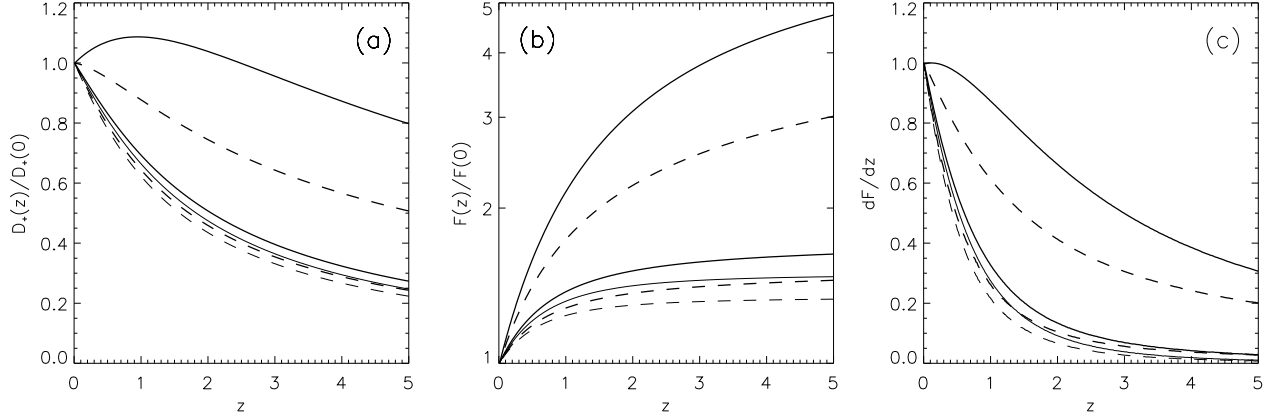


FIG. 2: (a) growth rate of matter density perturbations, (b) growth rate relative to Einstein-de Sitter and (c) differential growth rate per unit of redshift for two cosmological models with $w_x = -0.9$ and different dark energy fraction and interaction parameter. In all panels, solid lines correspond to $\Omega_x = 0.8$, and dashed lines to $\Omega_x = 0.7$. In each set and from top to bottom, the interaction parameter is $c^2 = 0.1, 0.01$, and 0 .

The ISW component cannot be measured directly, i.e., cannot be extracted from CMB data using frequency information since it has the same frequency dependence that any other intrinsic CMB signal. Since at low redshifts it is generated by local structures, the spatial pattern of ISW anisotropies will correlate with the matter distribution in the local Universe. The contribution to the radiation power spectrum due to the evolution of the gravitational potential at low redshifts is given by [31, 32]

$$C_l^{ISW} = \langle |a_{lm}|^2 \rangle = \frac{2}{\pi} \int_0^\infty k^2 dk P(k) I_l^2(k), \quad (4)$$

where

$$I_l(k) = 3\Omega_{c,0} \frac{H_0^2}{k^2} \int_0^{r_{rec}} dr j_l(kr) \frac{dF}{dr}. \quad (5)$$

In this expression, $F = D_+(z)(1+z)$ is the ratio of the growth of matter density perturbations in any cosmological model, $D_+(z)$, to that in a Einstein-de Sitter Universe, $(1+z)^{-1}$; H_0^{-1} is the present Hubble radius and $j_l(x)$ are spherical Bessel functions. In Figure 2 we plot the redshift evolution of D_+ , F and dF/dz . All the models have $w_x = -0.9$ and solid lines correspond to $\Omega_x = 0.8$ and dashed lines to $\Omega_x = 0.7$. From top to bottom, each group of lines corresponds to $c^2 = 0.1, 0.01$, and 0 , the latter pertaining to non-interacting models. The growth function was normalized to unity at $z = 0$, $D_+(0) = 1$.

Due to the ISW component, CMB temperature maps will correlate with tracers of the gravitational potential at low redshifts that could be constructed from galaxy catalogs. In particular, it will correlate with templates of the projected galaxy density along the line of sight. Assuming the distribution of galaxies follows that of the dark matter, the correlation of a template of projected galaxy density and a CMB map can be computed analytically [31],

$$C_l^{ISW-M} = \frac{2}{\pi} \int k^2 dk P(k) I_l^{ISW}(k) I_l^M(k), \quad (6)$$

with

$$I_l^M = \int_0^{r_0} dr W^M(k, r) j_l(kr), \quad (7)$$

where $W^M(k, r) = b(k, r) n_M(r) D_+(r)$ is the window function of the tracer of the large scale gravitational potential, $b(k, r)$ is the scale dependent bias existing between sources and the matter distribution as a function of radial distance r , $n_M(r)$ is the normalized redshift distribution of sources and $D_+(r)$ is the growth function of matter density perturbations. Similarly, the power spectrum of the galaxy catalog is given by

$$C_l^M = (2/\pi) \int k^2 P(k) (I_l^M(k))^2 dk. \quad (8)$$

One advantage of using Eq. (6) is that it separates the contribution coming from redshift evolution and from the spatial distribution of the large scale structure. Models of structure formation that give rise to the same matter power spectrum but differ in their growth rate, $D_+(z)$ (see Fig. 2b), will also give rise to ISW effects of different amplitude. Consequently, the correlation with galaxy catalogs will also differ. If the interaction varies with time and is only significant at present, the shape of the matter power spectrum will be unaffected but the growth rate will not. Therefore, the ISW effect will be sensitive to the existence of the interaction through the influence of the latter on the growth rate of density perturbations. In the next section, we shall fix the matter power spectrum of all models with interaction to be the same as a model with $c^2 = 0$ (no interaction) and the same cosmological parameters. We considered only power spectra that were compatible in amplitude and shape with the spectra derived from the SDSS and 2dGF galaxy catalogs [4]. Thus, differences in the correlation between templates of projected galaxy density and CMB data -Eq.(6)- will reflect differences in the growth ratio F only and will indicate how sensitive the ISW effect is to the redshift evolution of matter density perturbations.

III. OBSERVATIONAL PROSPECTS

After the release of WMAP 1yr data, several groups looked for evidence of ISW effect by cross-correlating the WMAP data with templates built from different catalogs: the NVSS radio survey [33, 34], the HEAO-I X-ray Background map [5], the APM [35], the SDSS [6, 36, 37], and the 2MASS galaxy surveys [38, 39]. These analyses rely on constructing templates from catalogs as tracers of the ISW signal. Cross-correlation of random realizations of CMB data and noise provides an estimate of the uncertainties. Catalogs differed in depth and sky coverage and different groups use different techniques: real space correlation, correlations in Fourier space, wavelets analysis, etc., and obtained positive detections with levels of significance of $2 - 4\sigma$. These detections represent an independent evidence for the existence of dark energy, though, at the moment, the measurements are not accurate enough to discriminate between competing dark energy scenarios.

In this section, we analyze the prospects that the ISW effect could be potentially sensitive to the growth rate of matter density perturbations and, therefore, to the dark energy-dark matter coupling. The effect of the interaction is to increase the amplitude of the cross-correlation of template and CMB data: the interaction makes the gravitational potentials decay faster which produces a larger ISW effect, making it easier to detect. If we trace the ISW effect with a template M that covers a fraction f_{sky} of the sky, the cumulative signal to noise ratio is given by [32]

$$\left(\frac{S}{N}\right)^2 = f_{sky} \sum_{l=2}^{l_{max}} (2l+1) \frac{(C_l^{ISW-M})^2}{(C_l^{ISW-M})^2 + (C_l^{CMB} C_l^M)}, \quad (9)$$

where C_l^M is the power spectrum of the template M . The sum extends to the largest angular scale resolved by the template. The main source of confusion in ISW measurements comes from the intrinsic CMB anisotropies. In Eq. (9) we have neglected the instrumental noise of WMAP data and the shot noise of the template map.

If the distribution of galaxies as a function of redshift is known, then the expected S/N ratio can be computed numerically. Following earlier practice, we model the redshift distribution of sources by the analytic expression, $n_M(z) = A(z/z_0)^2 \exp[-(z/z_0)^{3/2}]$. The constant z_0 measures the effective depth of the catalog and is simply related to the median redshift z_m of the source distribution, $z_m = 1.412 z_0$ [40, 41]. The normalization constant is

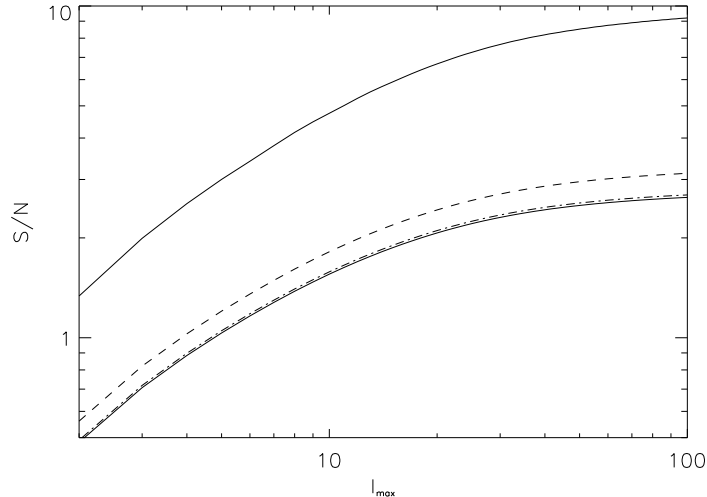


FIG. 3: Cumulative signal to noise ratio for a catalog with mean depth $z_m = 0.3$. From bottom to top lines correspond to $c^2 = 0$ (bottom thin-solid line), 10^{-3} (dot dashed line), 0.01 (dashed line), and 0.1 (solid line). Template and data are assumed to have full sky coverage.

fixed by setting $\int n_M(z)dz = 1$. In Fig. 3 we plot the cumulative S/N ratio for a cross-correlation of temperature data with a template constructed from a galaxy catalog with median redshift $z_m = 0.3$, as a function of the multipole l_{max} for 4 different interaction parameters. From bottom to top $c^2 = 0$ (bottom thin-solid line), 10^{-3} (dot dashed line, almost coincident with the previous one), 0.01 (dashed line), and 0.1 (solid line). For simplicity we considered data and template to have full sky coverage, i.e., $f_{sky} = 1$. In Fig. 3 it is seen that increasing the strength of the interaction augments the S/N ratio reflecting the fact that, as the interaction generates larger ISW signal, it can be detected with higher statistical significance.

Comparison between model predictions and observations can be done by means of the correlation function. The theoretical prediction is $\langle T * M \rangle(\theta) = \sum_l (2l+1) C_l^{ISW-M} P_l(\cos \theta) / 4\pi$. The cross-correlation of a template M constructed from a tracer of the large scale matter distribution like a galaxy catalog with a CMB map is simply

$$\langle T * M \rangle(\theta) = \frac{\sum_{(i,j) \in \theta} M_i T_j / \sigma_j^2}{\sum_{(i,j) \in \theta} 1 / \sigma_j^2}, \quad (10)$$

where M_i is the projected galaxy density on pixel i and σ_i is the noise associated to each pixel on a CMB map. The measured correlation function in Eq. (10) is affected by masking, pixelization and the inhomogeneities within the catalog of the galaxy selection function across the sky. Further, the free electrons that reside in the deep potential wells of galaxy clusters contribute to the temperature anisotropies via the thermal Sunyaev-Zeldovich (SZ) effect [42], that dilute the ISW signature at zero lag [6]. For example, templates constructed with the 2MASS catalog of galaxies are known to trace the thermal SZ component [43] as well the ISW effect. To avoid a possible thermal SZ contamination, we will compare the mean between 4 and 10° of the predicted and measured correlation functions. In Figure 4 we plot the correlation function computed using the analytic galaxy redshift distribution given above. Theoretical estimates were done assuming the bias factor b to be constant. Dashed lines corresponds to models with no interaction ($c^2 = 0$), $w_x = -0.9$ and three different dark energy densities: from bottom to top $\Omega_x = 0.7, 0.74$, and 0.8 . Solid lines correspond to interacting models with $c^2 = 10^{-3}, 0.01$, and 0.1 (from bottom to top), $w_x = -0.9$, and $\Omega_x = 0.74$. Full diamonds represent measurements of the ISW amplitude obtained by cross-correlating different galaxy catalogs with WMAP first year data (see [41] for details). For consistency with the data, the theoretical estimates are given in units of b . In the figure, the matter power spectra was normalized fixing the amplitude of the rms of matter density perturbations on a sphere of $8h^{-1}\text{Mpc}$ to be $\sigma_8 = 0.8$. As expected, if all models have the same σ_8 , the ISW effect increases with increasing Ω_x and increasing c^2 . The χ^2 per degree of freedom is less than 1, except for $c^2 = 0.01$, $\Omega_x = 0.74$ ($\chi_{dof}^2 = 1.5$) and $c^2 = 0$, $\Omega_x = 0.8$ ($\chi_{dof}^2 = 3.6$). An interaction parameter as high as $c^2 = 0.1$ is strongly ruled out by the observations, $\chi_{dof}^2 = 180$. The low quality of the fit is dominated by the

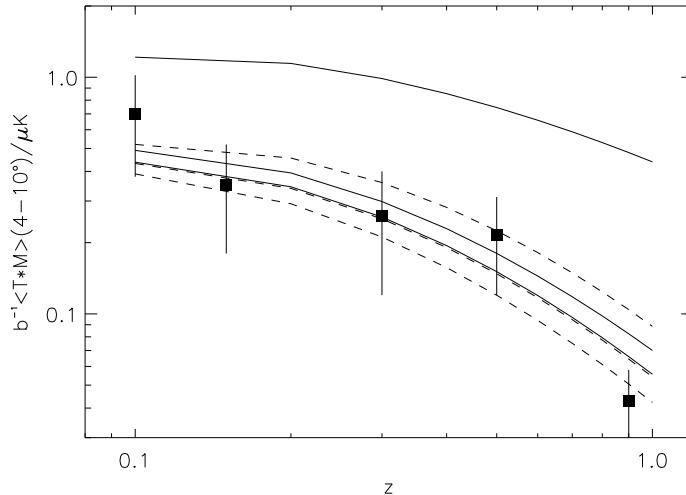


FIG. 4: Cross-correlation between CMB data and template, averaged on angular scales from 4 to 10° . Dashed lines corresponds to models with no interaction ($c^2 = 0$) and $w_x = -0.9$ and, from bottom to top: $\Omega_x = 0.7, 0.74$, and 0.8 . Solid lines correspond to interacting models (from bottom to top: $c^2 = 10^{-3}, 0.01$, and 0.1), $w_x = -0.9$, and $\Omega_x = 0.74$. Full diamonds represent the measurements obtained from different catalogs and their 1σ errors compiled in [41].

measurement at $z = 0.9$ obtained in [5] and derived using NVSS and HEAO-1 samples. Due to the systematic uncertainties of the bias and selection function in both samples, our simple model may not be accurate enough to make a meaningful prediction; but even if we disregard this data point, a value of $c^2 = 0.1$ can be ruled out at the 99.95% confidence level. The rejection level would be smaller if we considered the uncertainty in the shape of $n_M(z)$ and in the mean depth of galaxy catalogs. At any rate, this analysis shows that the ISW effect can effectively constrain the existence of an interaction at low redshift. It has more statistical power than the luminosity distance test based on SNIa observations [21].

If WMAP first year data showed a good agreement between the best fit values of Ω_x derived from the analysis of temperature anisotropy maps and those obtained by cross-correlating temperature maps with projected galaxy density templates, Cabré *et al.* [36, 40] noticed some tension between the values derived from these techniques using the less noisy WMAP third year data. The ISW signature of the new CMB data had a preference for larger values of Ω_x . The combined analysis of different samples gave $\Omega_x = 0.77 - 0.86$ at the 95% confidence level. The data was compatible with $w_x = -1$ (Λ CDM model), but did not have enough statistical power to break the degeneracy in the w_x vs Ω_x plane. Those results were later confirmed in [39] where a best fit value of $\Omega_\Lambda = 0.85$ for a flat Λ CDM model was reported, albeit with larger uncertainty. An interaction parameter of $c^2 \sim 0.01$ could produce a ISW signal similar to a non-interacting model with higher Ω_x , bringing back the agreement between the measured fraction of dark energy with WMAP 3yr data and with the ISW effect. Should the Cabré *et al.* or Rassat *et al.* results [36, 39, 40] be confirmed by deeper catalogs like the new SDSS releases or PanSTARRS [44], the ISW test will constitute an indirect evidence that the growth rate of matter density perturbations differs from that of the concordance Λ CDM model. Future surveys will be able to test different extensions of the standard model and prove/rule out the existence of an interaction.

IV. CONCLUSIONS

The ISW effect may provide an excellent tool to detect, in a model independent way, the coupling between dark energy and dark matter at low redshifts, i.e., $z \leq 1$. The interaction damps the growing mode of the Newtonian potential faster compared to models with no interaction and enhances the ISW effect; then, the ISW effect is sensitive to the growth rate of matter density perturbations, but model predictions need to be refined to model more realistically the selection function of galaxy catalogs. We have shown that the correlation of WMAP with templates constructed from different galaxy catalogs can rule out an interaction parameter of $c^2 = 0.1$ at better

than the 99.95% confidence level. For this type of models, this upper limit is stronger than those obtained previously using the CMB radiation power spectrum [19, 21], but at a different redshift. The ISW effect shows more statistical power to discriminate among IQM models than the luminosity distance test obtained using SNIa.

The recent results in [36, 40] suggest a discrepancy between the fraction of dark energy necessary to explain the amplitude of the ISW effect (measured from cross-correlating CMB data and galaxy catalogs) larger than allowed by the WMAP 3yr data. We have shown that the tension between both data sets could be explained by introducing a moderate coupling between dark energy and dark matter. This is in line with recent claims that the Layzer-Irvine equation [45] when applied to galaxy clusters reveals the existence of a DM/DE coupling [46]. If the aforesaid discrepancy is confirmed by deeper and wider galaxy samples, it could turn out an indirect evidence for the existence of a DM/DE interaction.

Acknowledgments

We are grateful to Wayne Hu for indicating us Refs. [26] and [27] as well as useful correspondence. This research was partly supported by the Spanish “Ministerio de Educación y Ciencia” (Grants FIS2006-12296-C02-01, BFM2000-1322 and PR2005-0359), the “Junta de Castilla y León” (Project SA010C05), and the “Direcció General de Recerca de Catalunya” (Grant 2005 SGR 00087).

-
- [1] S. Perlmutter *et al.*, *Nature* (London) **391**, 51 (1998); A.G. Riess *et al.*, *Astron. J.* **116**, 1009 (1998); S. Perlmutter *et al.*, *Astrophys. J.* **517**, 565 (1999); P. de Bernardis *et al.*, *Nature* (London) **404**, 955 (2000); R.A. Knop *et al.*, *Astrophys. J.* **598**, 102 (2003); J.L. Tonry *et al.*, *Astrophys. J.* **594**, 1 (2003); M.V. John, *Astrophys. J.* **614**, 1 (2004); A.G. Riess *et al.*, *Astrophys. J.* **607**, 665 (2004); P. Astier *et al.*, *Astron. Astrophys.* **447**, 31 (2006).
 - [2] D.N. Spergel *et al.*, *Astrophys. J. Suppl.* **170**, 377 (2007); G. Hinshaw *et al.*, *Astrophys. J. Suppl.* **170**, 288 (2007).
 - [3] M. Colless *et al.*, *Mon. Not. R. Astron. Soc.* **328**, 1039 (2001); M. Tegmark *et al.*, *Phys. Rev. D* **69**, 103501 (2004); V. Springel, C.S. Frenk, and S.M.D. White, *Nature* (London) **440**, 1137 (2006).
 - [4] S. Cole *et al.*, *Mon. Not. R. Astron. Soc.* **362**, 505 (2005).
 - [5] S.P. Boughn, and R.G. Crittenden, *Nature*, **427**, 45 (2004); S.P. Boughn, and R.G. Crittenden, *Mon. Not. R. Astr. Soc.* **360** 1013, (2005); S.P. Boughn, and R.G. Crittenden, *New Astron. Rev.* **49**, 75 (2005).
 - [6] P. Fosalba, E. Gaztañaga, and F.J. Castander, *Astrophys. J.* **597**, L89 (2003).
 - [7] C.R. Contaldi, H. Hoekstra, and A. Lewis, *Phys. Rev. Lett.* **90**, 221303 (2003).
 - [8] T. Padmanabhan, *Phys. Rep.* **380**, 235 (2003); V. Sahni, *Lect. Notes Phys.* **653**, 141 (2004); J.A.S. Lima, *Braz. J. Phys.* **34**, 194 (2004); L. Perivolaropoulos, *astro-ph/0601014*.
 - [9] P.J. Steinhardt, in *Critical Problems in Physics*, edited by V.L. Fitch and D.R. Marlow (Princeton University, Princeton, NJ, 1997).
 - [10] H. Martel, P.R. Shapiro, and S. Weinberg, *Astrophys. J.* **492**, 29 (1998); J. Garriga and A. Vilenkin, *Phys. Rev. D* **61**, 083502 (2000).
 - [11] E. Elizalde, *J. Phys. A: Math.Theor.* **40**, 6647 (2007).
 - [12] W. Zimdahl, D. Pavón, and L.P. Chimento, *Phys. Lett. B* **521**, 133 (2001).
 - [13] L.P. Chimento, A.S. Jakubi, D. Pavón, and W. Zimdahl, *Phys. Rev. D* **67**, 083513 (2003).
 - [14] C. Wetterich, *Nucl. Phys.* **B302**, 668 (1988).
 - [15] L. Amendola, *Phys. Rev. D* **62**, 043511 (2000); D. Tocchini-Valentini and L. Amendola *Phys. Rev. D* **65**, 063508 (2002); G. Farrar and P.E. J. Peebles, *Astrophys. J.* **604**, 1 (2004); S. Das, P.S. Corasaniti, and J. Khoury, *Phys. Rev. D* **73**, 083509 (2006); S. del Campo, R. Herrera, G. Olivares, and D. Pavón, *Phys. Rev. D* **74**, 023501 (2006).
 - [16] M.E. Soussa and R. P. Woodard, *Gen. Relativ. Grav.* **36**, 855 (2004); S. Nojiri and S. Odintsov, *Gen. Relativ. Grav.* **36**, 1765 (2004); S. Cappelzello, V.F. Cardone, and A. Troisi, *Phys. Rev. D* **71**, 043503 (2005).
 - [17] P.J.E. Peebles and B. Ratra, *Rev. Mod. Phys.* **75**, 559 (2003).
 - [18] K. Hagiwara *et al.*, *Phys. Rev. D* **66**, 010001 (2002).
 - [19] G. Olivares, F. Atrio-Barandela, and D. Pavón, *Phys. Rev. D* **71**, 063523 (2005).
 - [20] G. Olivares, F. Atrio-Barandela, and D. Pavón, *Phys. Rev. D* **74**, 043521 (2006).
 - [21] G. Olivares, F. Atrio-Barandela, and D. Pavón, *Phys. Rev. D* (2008) (in the press) arXiv: 0706.3860.
 - [22] L. P. Chimento and D. Pavón, *Phys. Rev. D* **73**, 063511 (2006).
 - [23] C. Di Porto, L. Amendola, *astro-ph/0707.2686*.

- [24] R.K. Sachs and A.M. Wolfe, *Astrophys. J.* **147**, 73 (1967).
- [25] C.P. Ma and E. Bertschinger, *Astrophys. J.* **455**, 7 (1995).
- [26] W. Hu and R. Scranton, *Phys. Rev. D* **70**, 123002 (2004).
- [27] W. Hu, *Astrophys. J.* **506**, 485 (1998).
- [28] J.K. Erickson *et al.*, *Phys. Rev. Lett.* **88**, 121301 (2002).
- [29] U. Seljak and M. Zaldarriaga, *Astrophys. J.* **469**, 437 (1996), see <http://www.cmbfast.org>
- [30] M.J. Rees and D.W. Sciama, *Nature*, **511**, 611 (1968); N. Aghanim, S. Majumdar and J. Silk, [arXiv:0711.051](https://arxiv.org/abs/0711.051).
- [31] R.G. Crittenden and N. Turok, *Phys. Rev. Lett.* **76**, 575 (1996).
- [32] A. Cooray, *Phys. Rev. D* **65**, 103510 (2002).
- [33] P. Vielva, E. Martínez-González, and M. Tucci, *Mon. Not. R. Astron. Soc.* **365**, 891 (2006); J. D. McEwen, P. Vielva, M. P. Hobson, E. Martínez-González, and A. N. Lasenby, *Mon. Not. R. Astr. Soc.* **373**, 1211 (2007).
- [34] M.R. Nolta, *Astrophys. J.* **608**, 10 (2004).
- [35] P. Fosalba and E. Gaztañaga, *Mon. Not. R. Astr. Soc.* **350**, L37 (2004).
- [36] A. Cabré, E. Gaztañaga, M. Manera, P. Fosalba, and F. Castander, *Mon. Not. R. Astr. Soc.* **372**, L23 (2007).
- [37] N. Padmanabhan *et al.*, *New Astron.* **9**, 329 (2004).
- [38] N. Afshordi, Y. Loh, and M. A. Strauss, *Phys. Rev. D* **69**, 083524 (2004);
- [39] A. Rassat, K. Land, O. Lahav, and F.B. Abdalla, *Mon. Not. R. Astr. Soc.* **377**, 1085 (2007).
- [40] A. Cabré, P. Fosalba, E. Gaztañaga, and M. Manera, [astro-ph/0701393](https://arxiv.org/abs/astro-ph/0701393).
- [41] E. Gaztañaga, M. Manera, and T. Multamäki, *Mon. Not. R. Astr. Soc.* **365**, 161 (2006).
- [42] R.A. Sunyaev and Ya.B. Zel'dovich, *Comments Astrophys. Space Phys.* **4**, 173 (1972); F. Atrio-Barandela and J.P. Mückel, *Astrophys. J.* **515**, 465 (1999); C. Hernández-Monteagudo, J.A. Rubiño-Martín, *Mon. Not. R. Astr. Soc.* **347**, 403 (2004).
- [43] C. Hernández-Monteagudo, R. Génova-Santos, and F. Atrio-Barandela, *Astrophys. J.* **613**, L89 (2004).
- [44] J.L. Tonry *et al.*, [astro-ph/07081364](https://arxiv.org/abs/astro-ph/07081364).
- [45] D. Layzer, *Astrophys. J.* **138**, 174 (1963).
- [46] O. Bertolami *et al.*, *Phys. Lett. B* (2008) (in the press); E. Abdalla *et al.*, [astro-ph/0710.1198](https://arxiv.org/abs/astro-ph/0710.1198).